# VACUUM MAGNETIC FIELD AND MODULAR COIL SYSTEM OF THE ADVANCED STELLARATOR WENDELSTEIN VII-AS

F. Rau, J. Kisslinger, H. Wobig

IPP 2/259 June 1982

MAX-PLANCK-INSTITUT FÜR PLASMAPHYSIK

8046 GARCHING BEI MÜNCHEN

MAX-PLANCK-INSTITUT FÜR PLASMAPHYSIK

GARCHING BEI MÜNCHEN

# VACUUM MAGNETIC FIELD AND MODULAR COIL SYSTEM OF THE ADVANCED STELLARATOR WENDELSTEIN VII-AS

F. Rau, J. Kisslinger, H. Wobig

IPP 2/259 June 1982

*Die nachstehende Arbeit wurde im Rahmen des Vertrages zwischen dem Max-Planck-Institut für Plasmaphysik und der Europäischen Atomgemeinschaft über die Zusammenarbeit auf dem Gebiete der Plasmaphysik durchgeführt.*

IPP 2/259

F. Rau
J. Kisslinger
H. Wobig

# Vacuum Magnetic Field and Modular Coil System of the Advanced Stellarator Wendelstein VII-AS

June 1982
(in English)

Abstract

The vacuum field and the modular coils of the advanced stellarator WENDELSTEIN VII-AS are described. Each of the five field periods contains 9 different twisted coils, one of them with increased dimensions and current in order to provide sufficient access. The standard vacuum field configuration (B = 3 T, $\iota$ = 0.39, aspect ratio $\approx$ 10, low shear, and magnetic well) can be varied by toroidal and vertical fields, or by changing independently the current in the large special coils. From a study of magnetic field perturbations some estimates are derived for the admissible coil tolerances.

CONTENTS

## INTRODUCTION

The present paper describes properties of the vacuum magnetic fields and the geometry of the modular coil system of the "Advanced Stellarator WENDELSTEIN VII-AS. The principles and methods of the theoretical optimization of stellarators are published elsewhere (1,2). In an advanced stellarator, and also in a "Reduced Q-Torsatron" (3), the poloidal variation of $\int d\ell/B$ (taken along one field period) is reduced in comparison to its value in the field of a classical stellarator with identical rotational transform and aspect ratio. Then the following three quantities are simultaneously reduced:

i) the offset of drift-surfaces of passing particles from the magnetic surfaces,

ii) the magnitude of the secondary plasma currents, and

iii) the SHAFRANOV-shift of the magnetic surfaces caused by a finite plasma pressure.

As a consequence of i) and ii), in the regimes of collisional and plateau diffusion,the particle loss rate is reduced, as shown by a Monte-Carlo-computation of the diffusion coefficient (4,5).

In WENDELSTEIN VII-AS these reductions amount to factors of about two, within the range of experimental flexibility (5-9). Such apparently moderate factors are the result of the optimization procedure (2), in which the existence of a magnetic well and a low plasma aspect ratio are favoured against a further reduction of the poloidal variation of $\int d\ell/B$.

For the development of the modular coil set of WENDELSTEIN VII-AS the advanced stellarator configuration ASC 742 - obtained (2) by A. SCHLÜTER - is chosen as initial magnetic topology. This configuration has a plane non-circular magnetic axis and 5 field periods. It allows a smaller coil aspect ratio than the similar configuration ASC 084 with 10 field periods. The magnetic topology of ASC742 is improved by W. DOMMASCHK in the configuration WAD 500, towards a smaller magnetic field ripple.

The topologies of these advanced stellarator configurations are given as a series of DOMMASCHK-potentials (10), from which the magnetic fields and flux surfaces, etc. are computed numerically. The currents to produce the magnetic field topologies can be obtained by a separate procedure (11) as a surface current distribution on a given torus. Comparatively low toroidal excursions of the current lines are found if this torus is not too far outside of the magnetic surfaces, especially if its cross section is matched approximately to their shape. Typically 8 current lines per field period are sufficient to reproduce the configuration reasonably (2).

MODULAR COIL SYSTEM

The modular coil system of WENDELSTEIN VII-AS is developed by a discretization of the surface current pattern of ASC 742. This development is carried out during several empirical steps, where the effort is directed to match requirements which are not included in the numerical procedures for finding the DOMMASCHK-potentials and the associated surface currents. These modifications could be performed without essentially impairing the favourable advanced stellarator properties. Their major steps are:

i) an analytical approximation of the numerical surface current distribution of ASC 742, the resulting configuration JOK 571 being characterized by 10 different filamentary current lines per field period on a torus with variable major radius, aspect ratio, and prolate ellipticity;

ii) an optimization of the torus topology in order to increase the available space for the vacuum tank, by using the data set JOK 744 derived from JOK 571 in an iteration which is detailed below;

iii) the final choice of a total of 9 different twisted coils per field period, where one of them is a large special coil with increased dimensions and current, and with a different shape, in order to provide sufficient access to the system without introducing too much magnetic ripple in the field topology;

iv) a further increase of the minimum radii of curvature of the twisted coils to facilitate their construction and a fine-tuning of their position in order to match estimated tolerances of the coils and the vacuum vessel.

The aims for the modification of ASC 742 and JOK 571 were the following: reduction of the magnetic field variation close to the magnetic axis, and improving the access for neutral beam injection. These aims are attained in the coil configuration AS 777 which uses 5 current filaments for each of the 10 twisted coils per field period. This coil configuration contains some gap near the middle of each field period, and the resulting magnetic ripple is compensated by an additional large planar coil. The size of this gap is increased by combining the two twisted coils near the middle of the field period and the large planar coil to one large special coil of a different twisted shape with increased dimensions and current. This data set is labelled AS 777 ML. In order to also increase the dimension of the vacuum tank, a data set AS 777 OL without a gap near the middle of the field period is derived, which again uses 10 twisted coils per field period. The magnetic field computed numerically from this coil set is then transferred to a series of DOMMASCHK-potentials, yielding the configuration JOK 744.

For this data set and therefore without changing the magnetic topology, by the use of the procedure described in (11), different surface current patterns are computed on tori chosen with differing size or shape, in order to optimize the distance between the last useful flux surface of the configuration and the torus of the field producing surface currents.

As result of this study the surface current distribution of JOK 744 finally is chosen on a torus with prolate elliptical cross-section, at a toroidally variable major radius

$$R_o(\varphi) = 200\,(1.02 - 0.03\cos 5\varphi), \qquad (1)$$

where the orientation of the half-axes $a_o = 41.5$ cm and $b_o = 56$ cm oscillates simultaneously in the poloidal direction by an angle

$$\theta_o(\varphi) = -\pi/8\,(\sin 5\varphi + 0.5 \sin 10\varphi), \qquad (2)$$

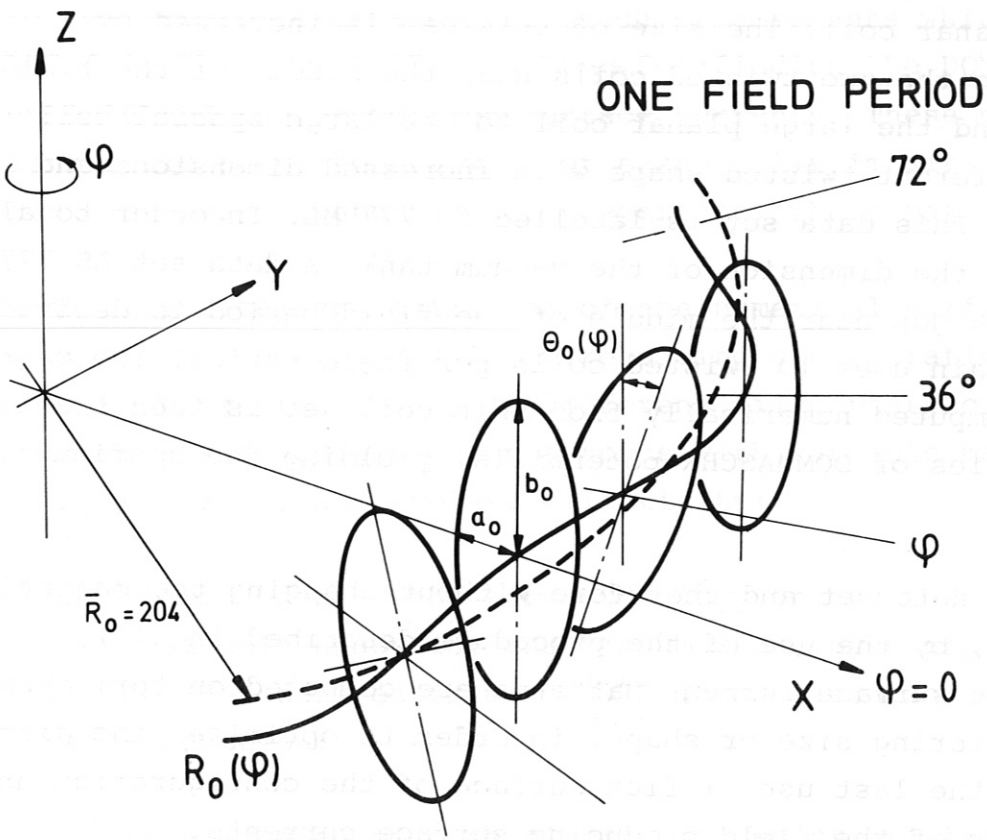


Fig. 1: Toroidal geometry of the surface current distribution used for the development of the modular coils for WENDELSTEIN VII-AS

see Fig. 1. For the bore of the twisted coils of WENDELSTEIN VII-AS - except for the large special ones which are described below - we consider a torus as specified in eq. 1) and 2), but reduce the half axes $a_o$ and $b_o$ by 9.2 cm, which is half of the height of the twisted coils.

This torus geometry is found to be an optimum considering a maximum distance between the plasma and the wall of the vacuum tank, along with the constraints of keeping the toroidal excursions and local radii of curvature of the twisted coils within technical limitations.

After this optimization procedure the surface current distribution is transferred to a system of discrete coils. Also the special coils for neutral beam injection are introduced. The magnetic field of JOK 744 represented in DOMMASCHK-potentials agrees well with that of the real coil system, except for the moderate extra ripple caused by the special injection coils.

In Fig. 2, the surface current distribution of JOK 744, and the contours of the bore of the twisted coils of WENDELSTEIN VII-AS are compared in an angular projection. The ordinate is the poloidal angle, and the abscissa is one field period of the toroidal angle. Both patterns agree reasonably.

Fig. 3 is a top view on one field period of the coil system of WENDELSTEIN VII-AS. There are eight twisted coils of identical prolate elliptical bore cross-section with differing orientation according to eq. (2). The current center of these coils is situated close to the torus specified above, at an average minor radius $\sqrt{a_o b_o} \approx 48$ cm. The design current is 592 kA-turns, and the rectangular coil cross-section (width = 12 cm, height = 18.4 cm) corresponds to a gross current density of about 2.7 kA/cm$^2$, including insulation and cooling-water channels.

The large special coil in the middle of the field period is clearly visible. Its major radius position $R_s = 224.5$ cm as well as its twisted shape are found by trial and error, and ensure a near-tangential access to the system with a sufficiently large aperture for neutral beam heating. It has a bore with

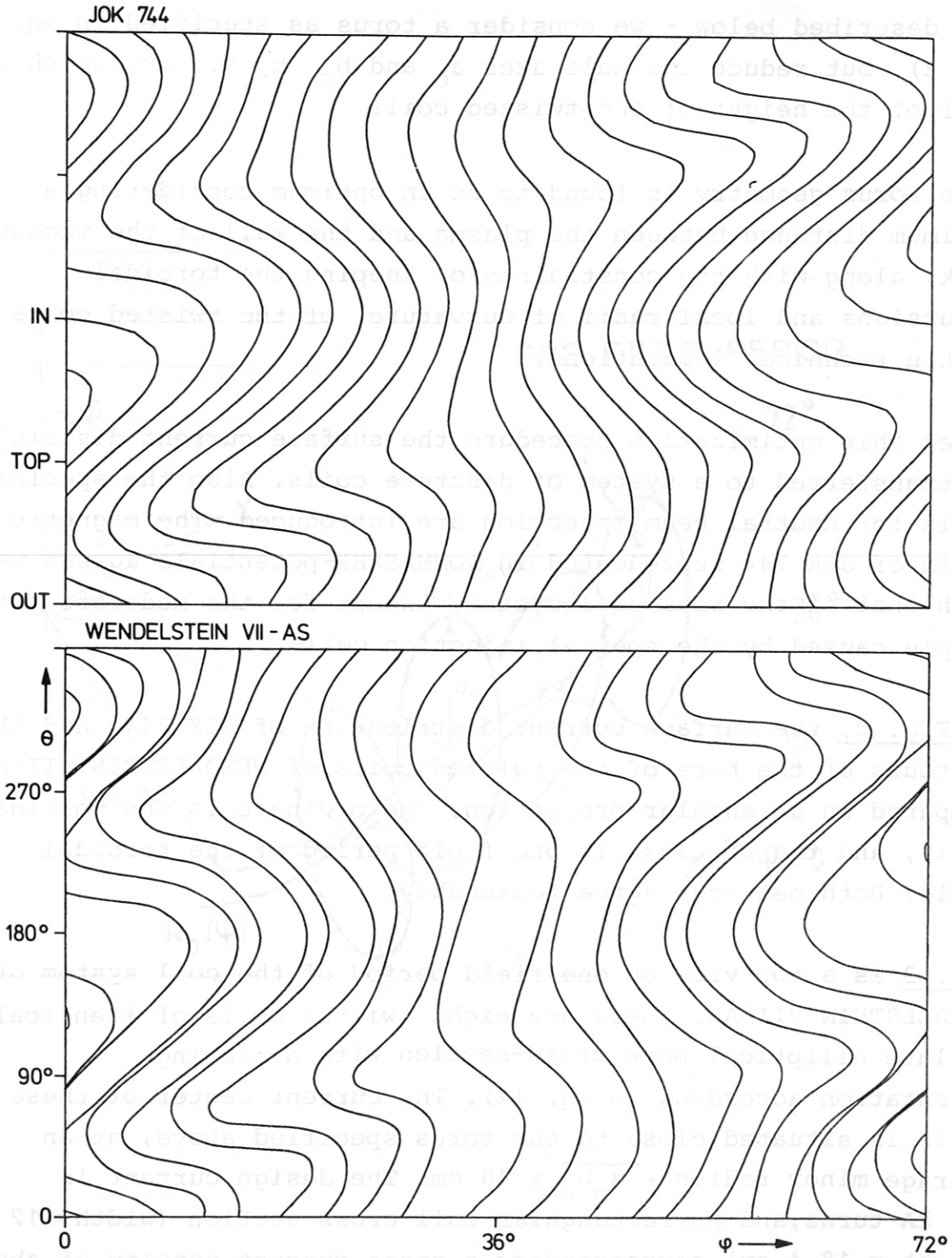


Fig. 2: Angular projections of surface current distribution JOK 744 (upper part), and contours of the bore of the twisted coils of WENDELSTEIN VII-AS (lower part). Abscissa = one field period, ordinate = one poloidal transit.

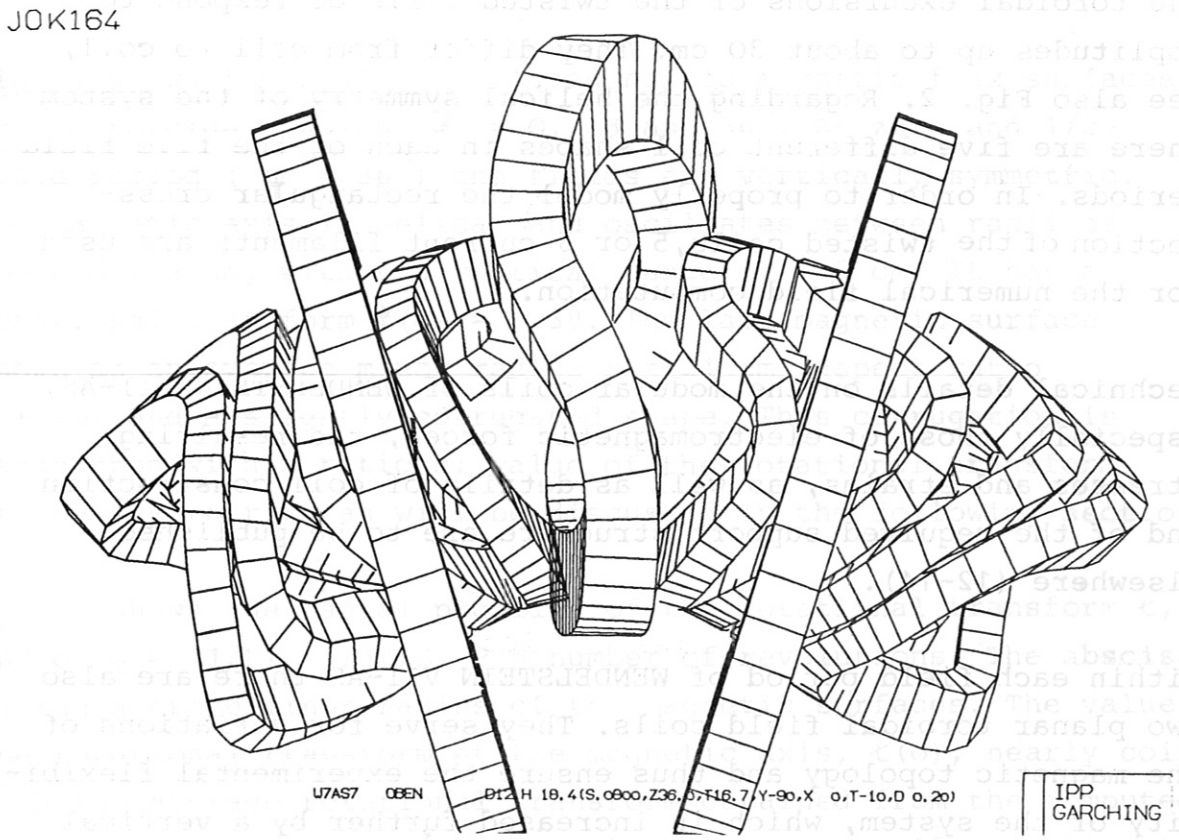


Fig. 3: Top view of coil system of WENDELSTEIN VII-AS, one field period containing 9 twisted coils and two planar toroidal field coils.

threefold poloidal periodicity, with one tip pointing radially outwards. The minor radius of its current center varies between 61.5 and 73 cm. The coil width is 21 cm and the coil height is 28 cm. The design current is 1.48 MA-turns.

The toroidal excursions of the twisted coils correspond to amplitudes up to about 30 cm. They differ from coil to coil, see also Fig. 2. Regarding the helical symmetry of the system there are five different coil shapes in each of the five field periods. In order to properly model the rectangular cross-section of the twisted coils, 5 or 6 current filaments are used for the numerical field computation.

Technical details on the modular coils of WENDELSTEIN VII-AS, especially those of electromagnetic forces, the resulting stresses and strains, as well as details of coil construction and of the required support structure are to be published elsewhere (12-14).

Within each field period of WENDELSTEIN VII-AS there are also two planar toroidal field coils. They serve for variations of the magnetic topology and thus ensure the experimental flexibility of the system, which is increased further by a vertical field, and by the possibility to change independently the current in the large special coils.

## STANDARD CASE OF MAGNETIC CONFIGURATION

Using the twisted coils of WENDELSTEIN VII-AS with the design currents as given above, the "standard case" of the magnetic field amounts to an induction of B = 3 T, at a major radius of about 2 m.

Fig. 4 shows the system of closed nested magnetic flux surfaces at the toroidal angles $\varphi$ = 0, 18 and 36°. At zero and 1/2 field period ( $\varphi$ = 36°) the fields are vertically symmetric. The magnetic axis is helical and oscillates between radii of 200 and 213 cm, within a vertical range of ± 2 cm. It has a rotational transform $\iota(0)$ = 0.39. The last magnetic surface shown as an average minor radius r = 21 cm (aspect ratio A ≈ 10) and a slightly corrugated shape. This corrugation is associated with a rational value of the rotational transform at the separatrix, as will be discussed in the following section.

Fig. 5 shows the radial profiles of the rotational transform $\iota$, and of $q = (1/P) \cdot \int d\ell/B$, P = number of revolutions. The abscissa is the average minor radius of the magnetic surfaces. The value of the rotational transform at the magnetic axis, $\iota(0)$, nearly coincides with the average rotational transform obtained from the computed magnetic surfaces. The minimum value is near r = 15 cm; close to the last magnetic surface $\iota$ increases again. The shear

$$\delta\iota/\iota(0) = (\iota(r) - \iota(0)) / (\iota(0) \qquad (3)$$

is below 1 %.

There exists a magnetic well within the whole range of flux surfaces

$$\delta V'/V' = (q(r) - q(0))/q(0) \qquad (4)$$

which increases towards $V'' \approx -2$ % for the last surface.

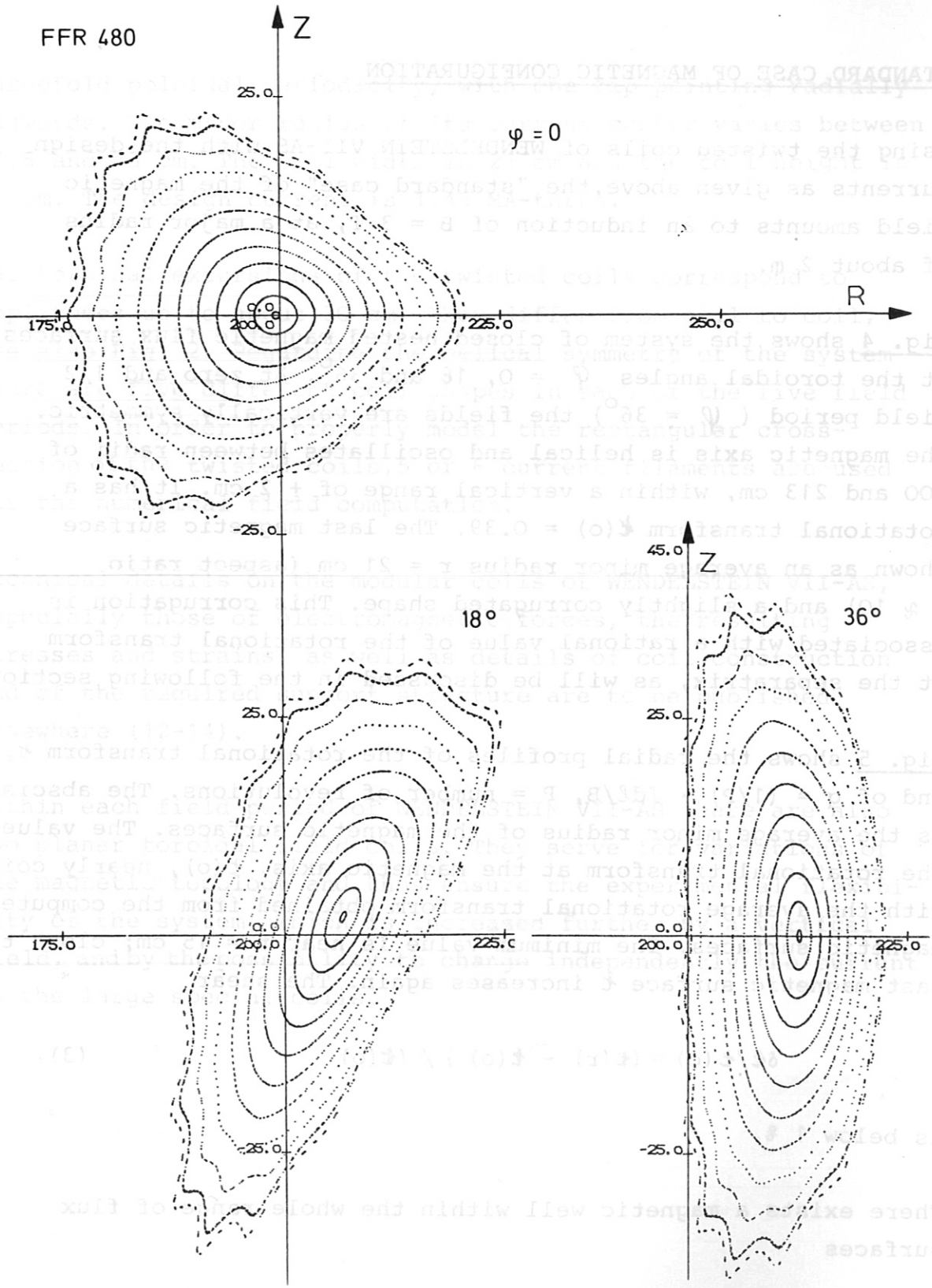


Fig. 4: Magnetic vacuum field with nested system of flux surfaces for WENDELSTEIN VII-AS at the toroidal positions $\varphi$ = 0, 18 and 36° corresponding to zero, 1/4 and 1/2 field periods; "standard configuration"

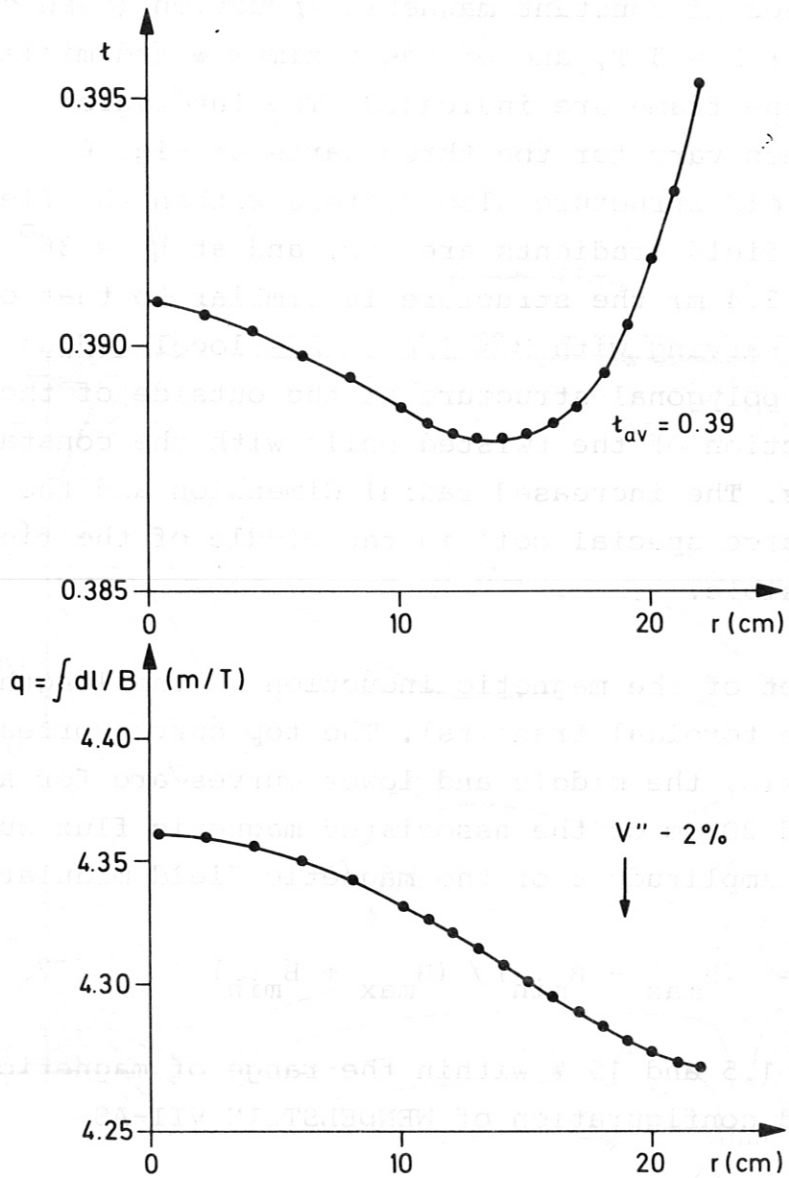


Fig. 5: Radial profiles of the rotational transform $\iota$ and of $q \sim \int d\ell/B$ for the flux surfaces of Fig. 4.

The Figs. 6a - 6c show for the same toroidal positions as Fig. 4 the contour lines of constant magnetic induction (dashed lines). The positions of B = 3 T, and of the maximum ● and minimum o values within the frame are indicated. The intervals between the contour lines vary for the three parts of Fig. 6.
The magnetic field structure also differs within the field period. At $\varphi$ = 0 the field gradients are low, and at $\varphi = 36^{\circ}$ (Fig. 6c, left part, r < 2.4 m) the structure is similar to that of a toroidal field varying with $B \sim 1/\rho$ , $\rho$ = local radius of curvature. The polygonal structure at the outside of the plots is the intersection of the twisted coils with the constant toroidal angles. The increased radial dimension and the different shape of the large special coil in the middle of the field period are clearly visible.

Fig. 7 is a plot of the magnetic induction vs the length of the field line (two toroidal transits). The top curve corresponds to the magnetic axis, the middle and lower curves are for average radii of 10 and 20 cm of the associated magnetic flux surfaces of Fig. 4. The amplitude $\delta$ of the magnetic field modulation,

$$\delta = (B_{max} - B_{min}) / (B_{max} + B_{min}) \qquad (5)$$

varies between 1.5 and 15 % within the range of magnetic surfaces of the standard configuration of WENDELSTEIN VII-AS.

The spatial structure of the magnetic field is visualized again by plotting the trace of the field line and contours of constant magnetic induction versus the toroidal and poloidal angles. This is shown for the magnetic flux surface with an average radius r = 10 cm in Fig. 8. The abscissa corresponds to one field period, and the ordinate to one poloidal transit, with top and bottom of the figure at the radial outside. The trace of the field line (upper part) exhibits the structure typical for stellarators: the rotational transform results as the average increase of the poloidal angle, when progressing along the undulating trace in the toroidal direction.

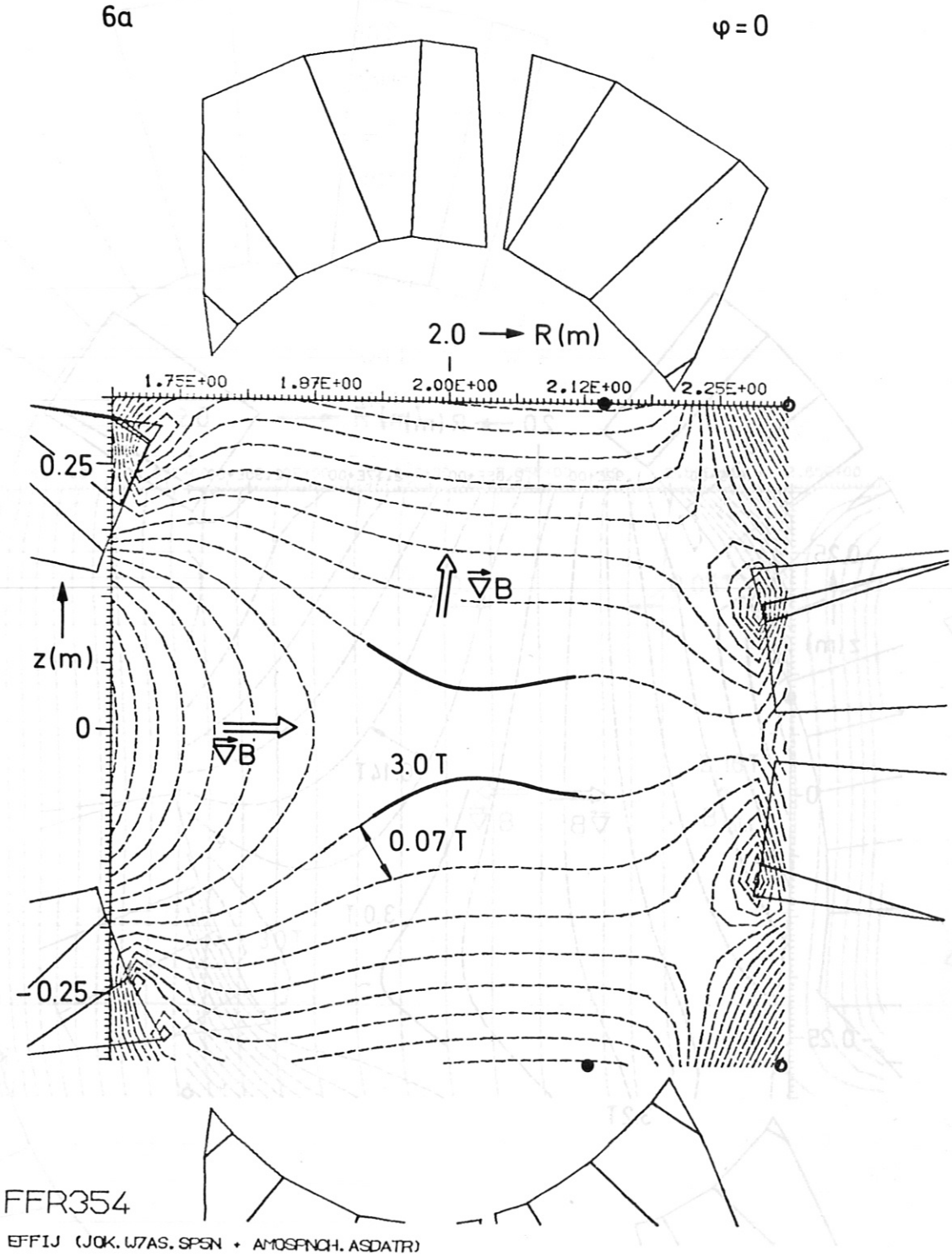


Fig. 6: Contours of constant magnetic induction (dashed) and intersections of some of the twisted coils with the toroidal angles $\varphi$ = 0, 18 and 36°; (Fig. 6a, 6b, 6c)

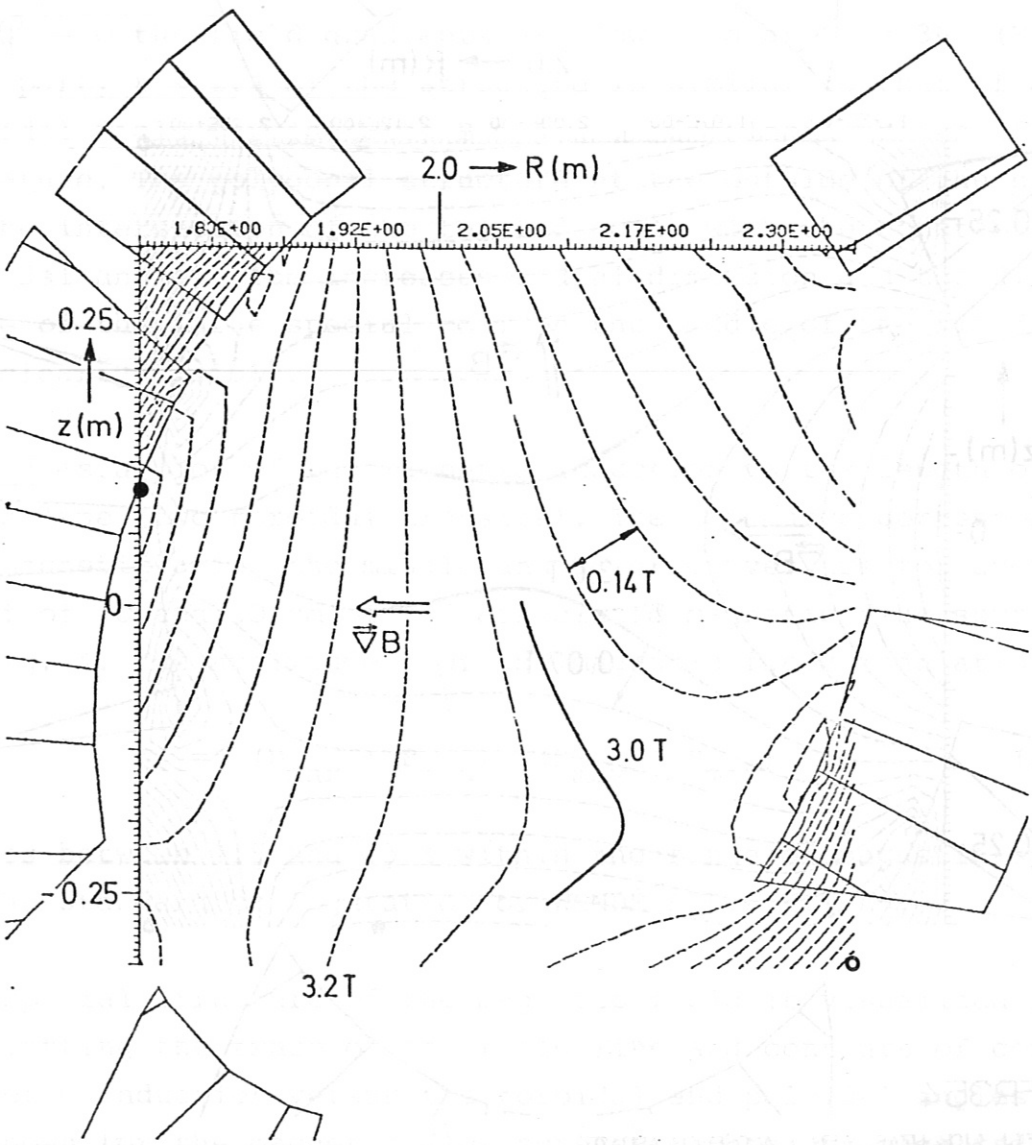


Fig. 6b: $\varphi = 18^{\circ}$ , 1/4 field period

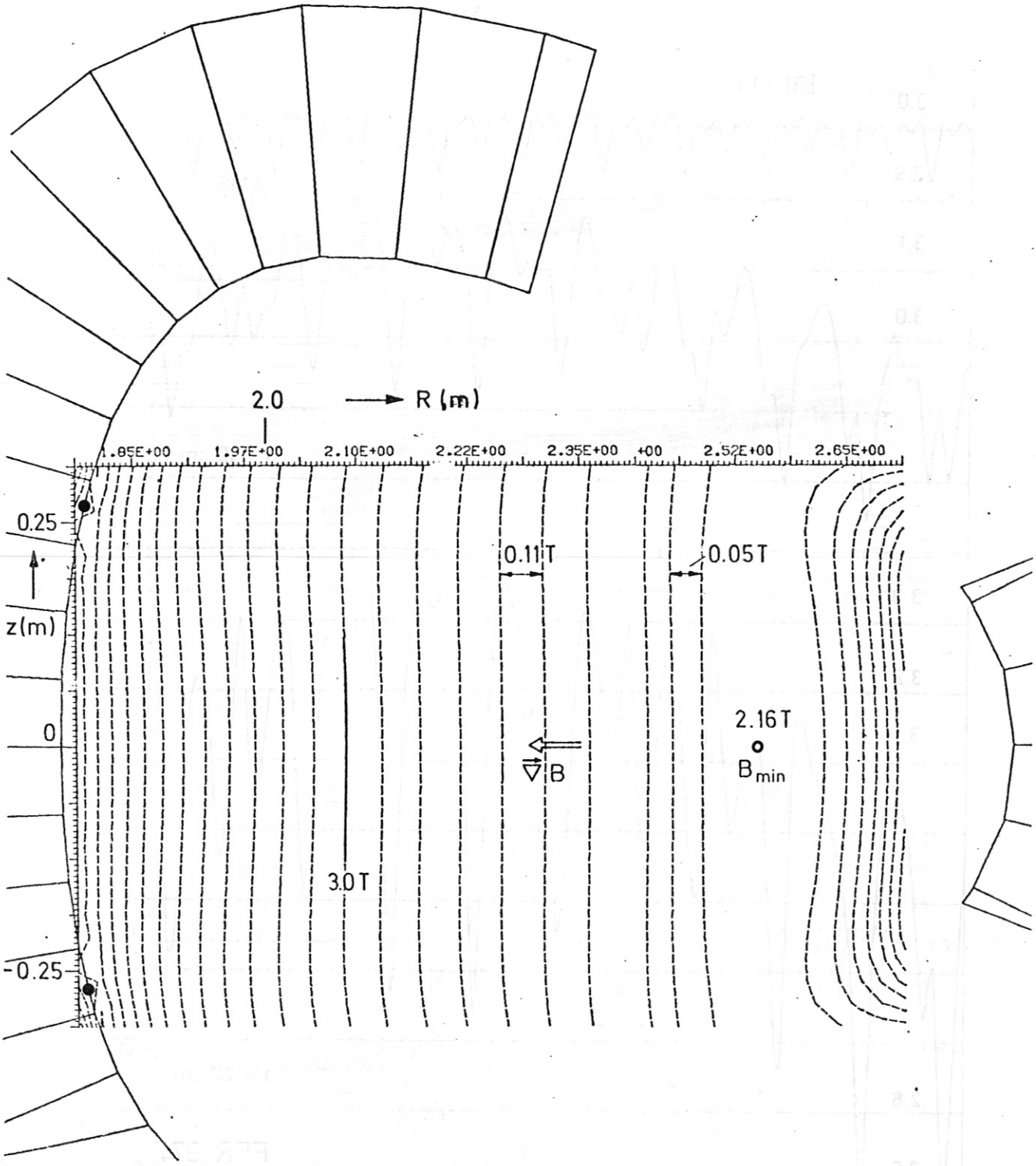


Fig. 6c: $\varphi = 36^{\circ}$ , 1/2 field period

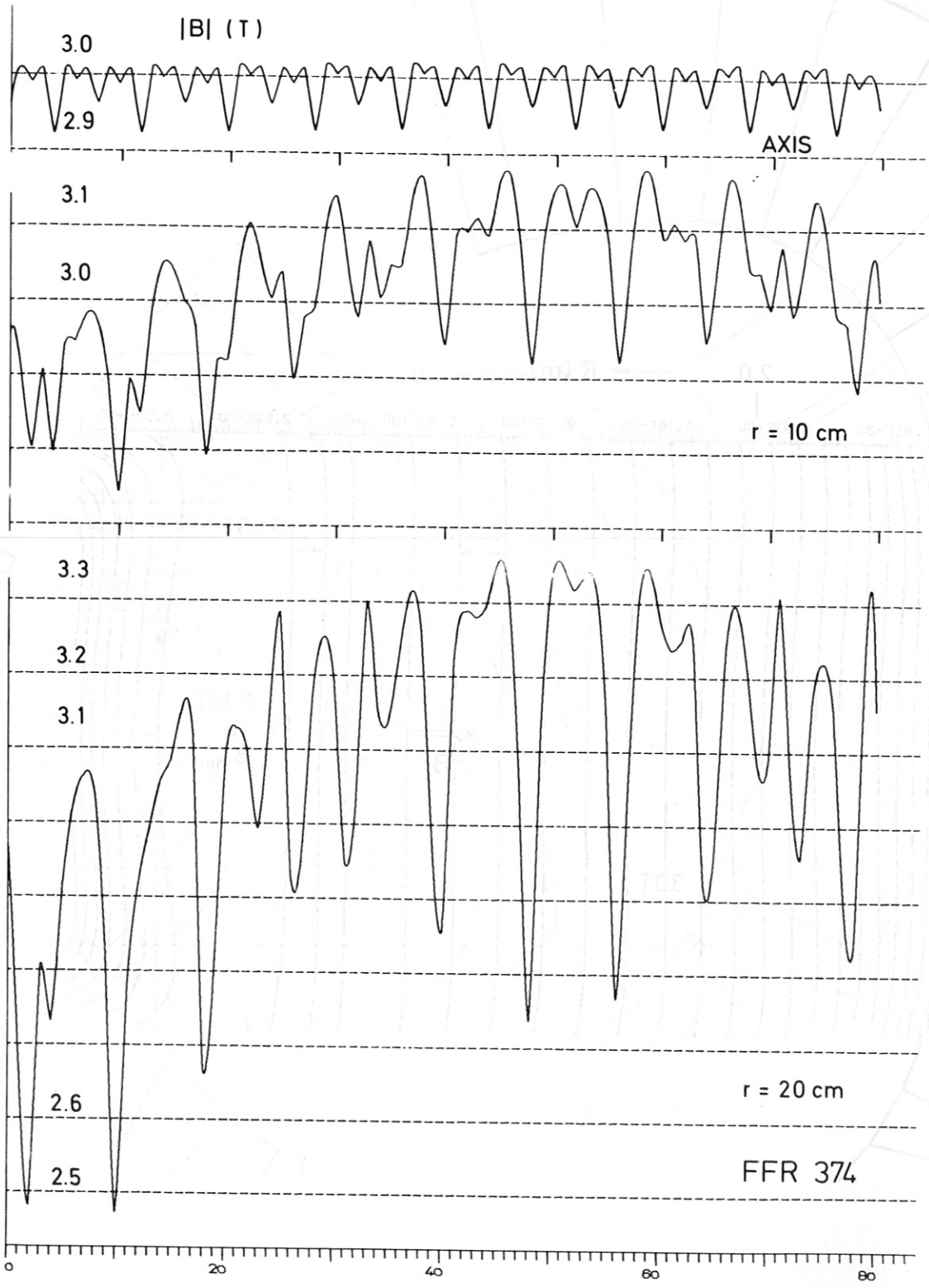


Fig. 7: Magnetic induction vs length of the field line for the magnetic axis and two flux surfaces at average radii of r = 10 and 20 cm (top to bottom).

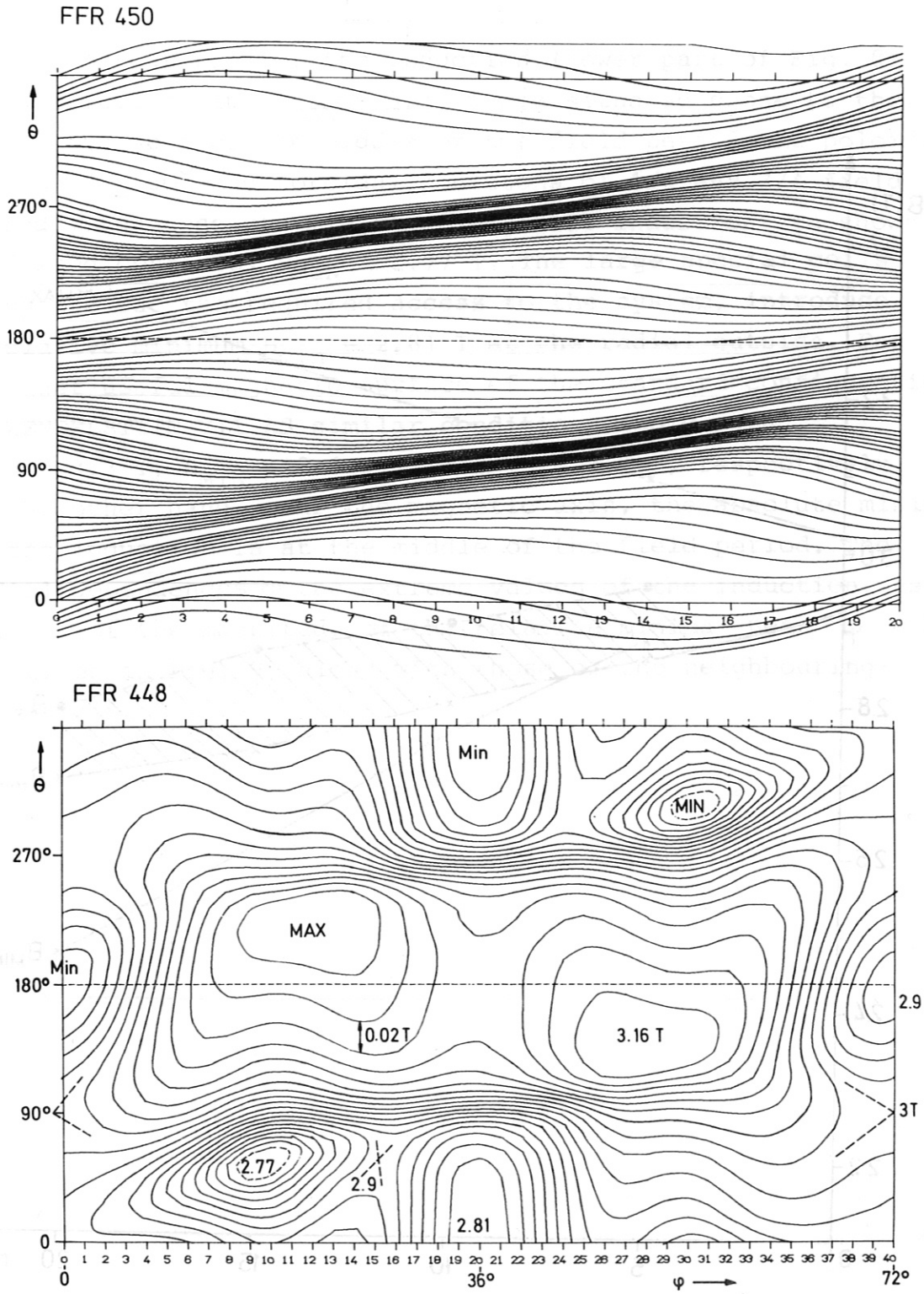


Fig. 8: Trace of the magnetic field line and contour plot of magnetic induction for the magnetic surface with an average radius of 10 cm, in an angular projection as Fig. 2.

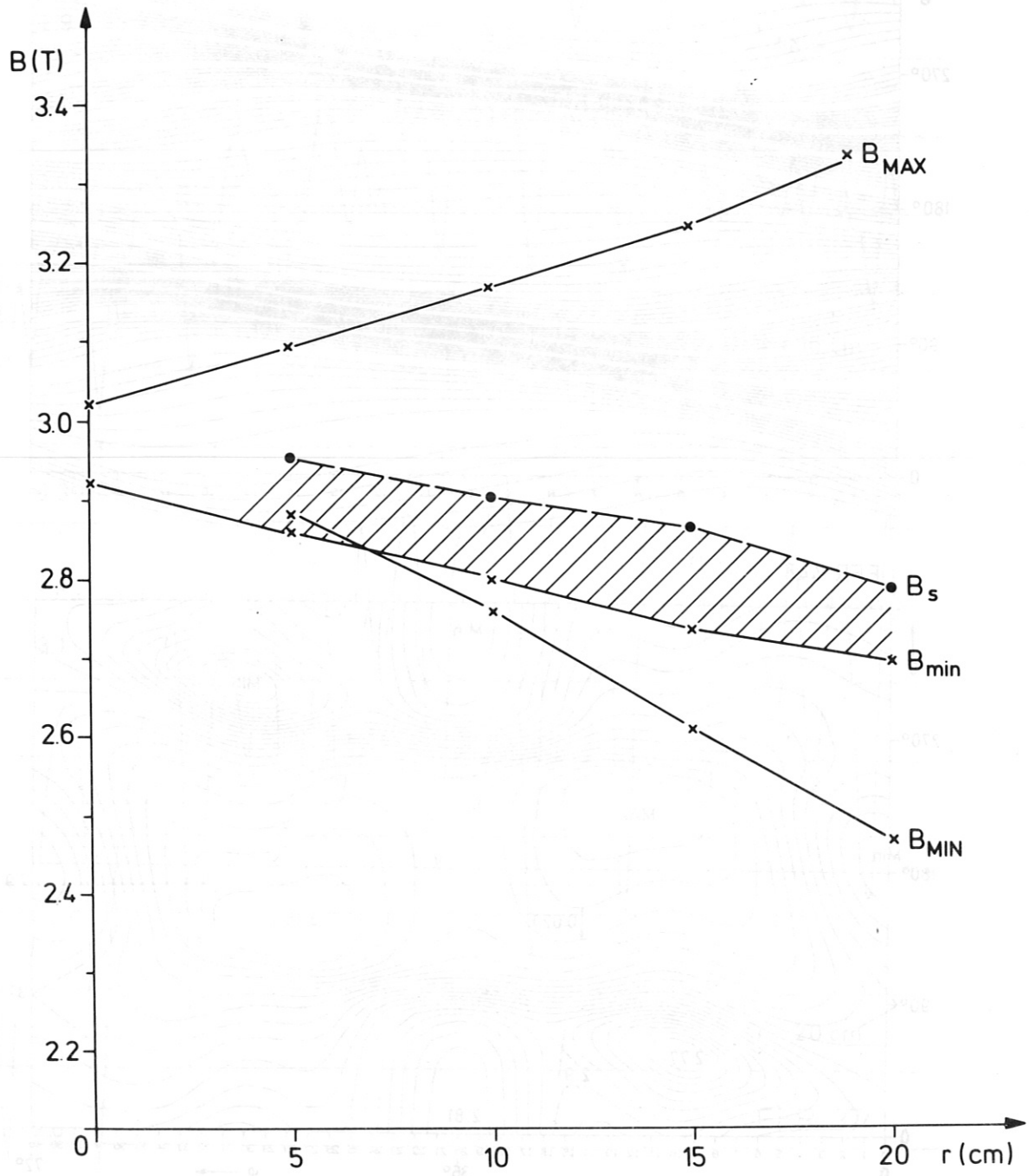


Fig. 9: Extreme values of the induction versus average radius of magnetic surfaces.

In the contour plot of the induction (lower part of Fig. 8) two absolute maxima $B_{MAX}$ = 3.16 T are situated close to the radial inside near the middle of the field period. At poloidal angles of $\pm$ 60° and toroidal positions of 1/4 and 3/4 field periods, the absolute minima of magnetic induction are shown as dashed contours, $B_{MIN}$ = 2.77 T. The large special coils, which provide the required access to the system, introduce a relative minimum $B_{min}$ = 2.81 T at the radial outside. For the last useful magnetic surface of the standard configuration of WENDELSTEIN VII-AS similar conditions apply with $B_{MAX}$ = 3.3 T, $B_{MIN}$ = 2.4 T, and $B_{min}$ = 2.7 T, respectively. On the other hand, near the magnetic axis, the absolute minimum of the induction is at the middle of the field period. The radial dependences of the extreme values of the induction, as well as of the magnitude of the relative minima near $\varphi$ = 36° are given in Fig. 9, along with those of the neighbouring separatrix, $B_s$.

PARAMETER VARIATION

The magnetic field topology of WENDELSTEIN VII-AS can be varied by several independent means, in order to establish the required experimental flexibility:

i) superposing toroidal fields up to ± 0.5 T from the system of 10 toroidal field coils, with an associated change of the rotational transform between $0.2 < \iota < 0.6$, see Fig. 10;

ii) superposing a vertical field of ± 0.05 T which changes $\iota$ but mainly shifts the magnetic axis and changes the magnetic well depth towards a magnetic hill at a large inside shift, especially in a case where the rotational transform of the resulting configuration is matched to the value of the standard configuration, see Fig. 11.

iii) adjusting the current in the large special coils independently from the current in the other twisted coils, which increases the magnitude of the magnetic ripple, see Fig. 12 (thus influencing the behaviour of trapped particles), and reverses the positions of the absolute and relative minimum of the induction at 1/4 and 1/2 field periods of the outer magnetic surfaces.

By further adjustment of the current in the 10 planar TF coils, either the average induction or the rotational transform can be matched to the respective values of the standard configuration, as listed in Table I.

For these three types of parameter variations of WENDELSTEIN VII-AS its quality of an "advanced stellarator", i.e. the low poloidal variation of $\int d\ell/B$, is essentially maintained.

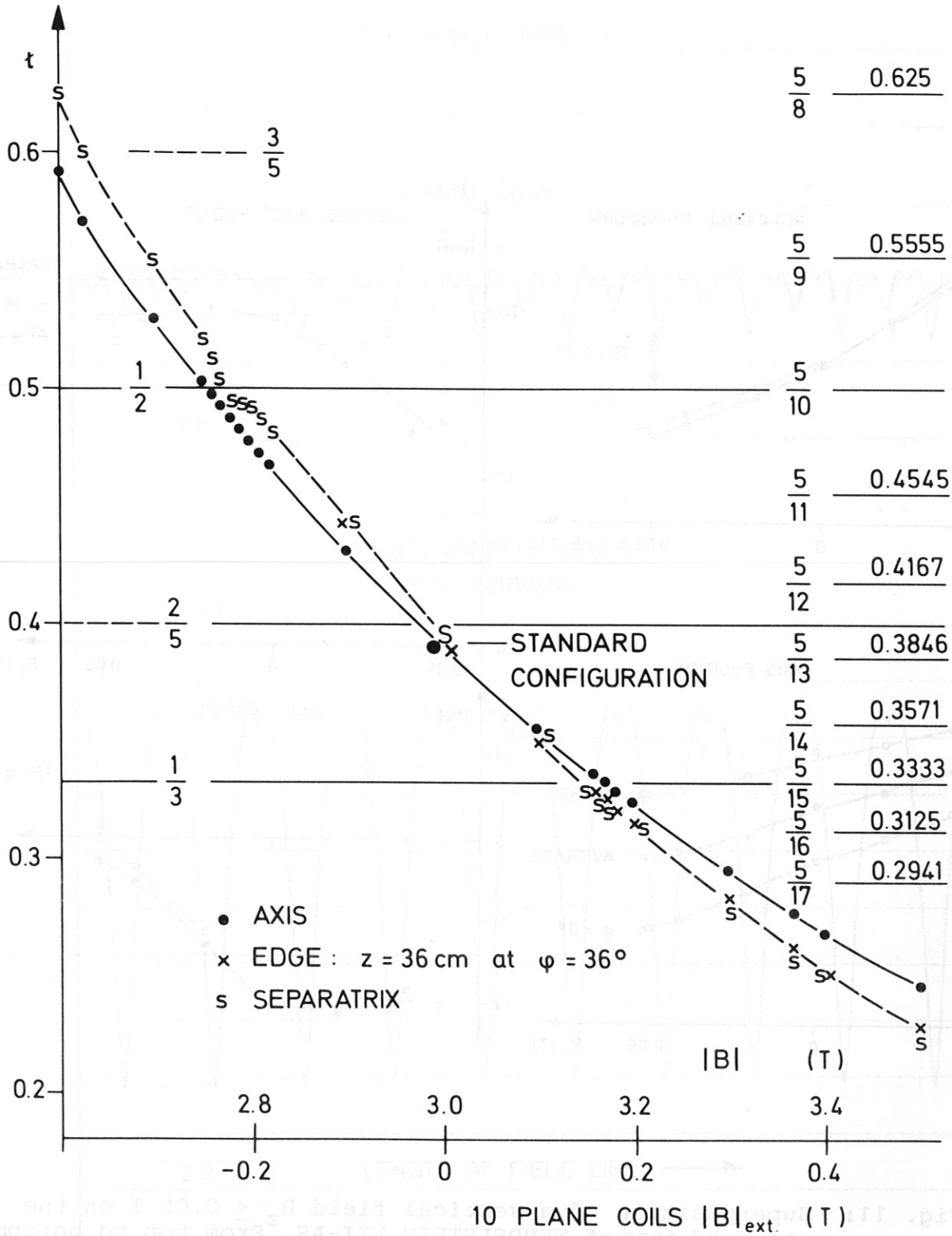


Fig. 10: Dependence of rotational transform $\iota$ on a toroidal field up to ± 0.5 T superposed from 10 planar TF-coils to the field of the standard case B = 3 T, as produced by the twisted coils.

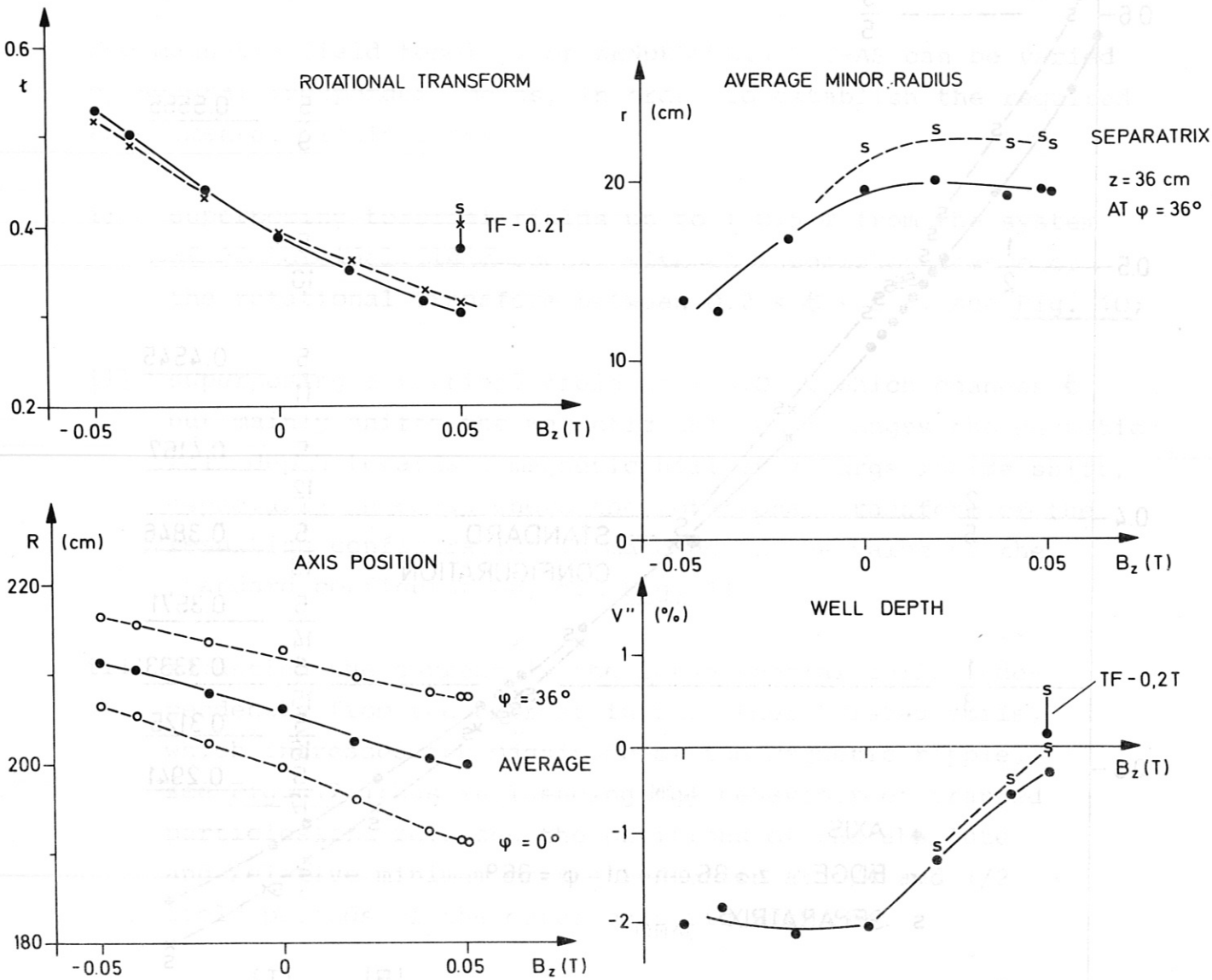


Fig. 11: Superposition of a vertical field $B_z \leq 0.05$ T on the standard case of WENDELSTEIN VII-AS. From top to bottom : rotational transform, position of the magnetic axis, average radius of the last useful magnetic surface, and magnetic well depth. An additional toroidal field of - 0.2 T matches the rotational transform of a configuration with a magnetic hill to that of the standard case at $B_z = 0.05$ T.

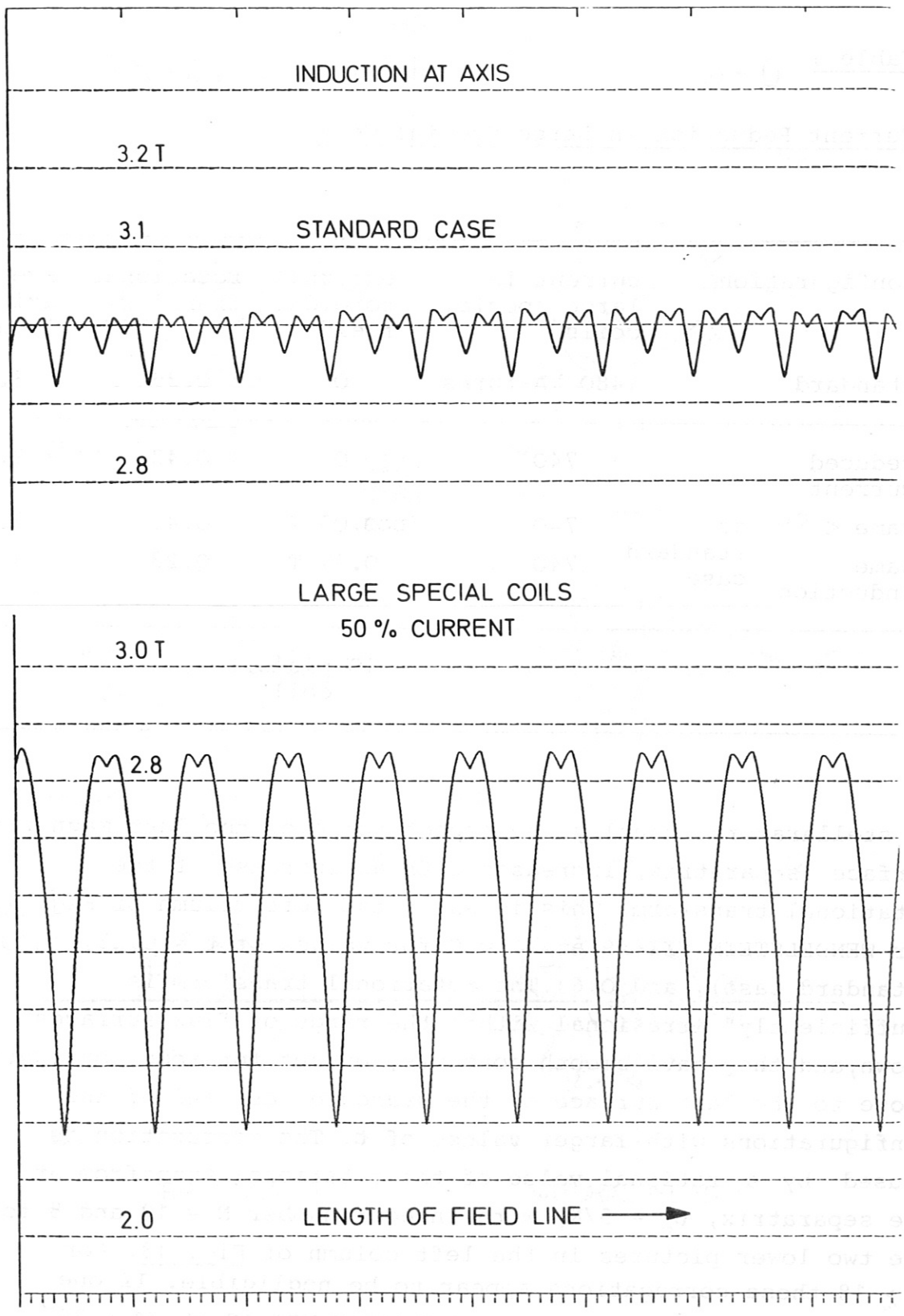


Fig. 12 : Magnetic induction at the axis vs length of the field line. From top to bottom : standard case; current in the large special coils reduced to 50 % of the design value.

Table I

Current Reduction in Large Special Coils

| configuration | current in large special coils | external toroidal field | rotational transform | average axis induction |
|---|---|---|---|---|
| standard | 1480 kA-turns | 0 | 0.39 | 3.0 T |
| reduced current | → 740 | 0 | → 0.43 | → 2.6 T |
| same $\iota$ as standard case | 740 | 0.05 T | 0.4 | 2.6 |
| same induction | 740 | 0.37 T | 0.28 | 3.0 T |
| | | 10 planar coils | | |

In stellarators, usually the aspect ratio of the last magnetic surface (separatrix) increases with an increase of the rotational transform. This is shown the left column of Fig. 13 for WENDELSTEIN VII-AS, at $\varphi$ = 0 for values of $\iota$ = 0.23, 0.39 (standard case), and 0.61. The rotational transform is "sufficiently" irrational within the range of flux surfaces shown, and they have smooth contours, except for some corrugation close to the last surface of the standard case and of the configurations with larger values of $\iota$. The corrugation is caused by a rational value of the rotational transfrom at the separatrix, $\iota_s$ = 5/N, with integer number N = 12 and 8 for the two lower pictures in the left column of Fig. 13. For $N \gtrsim 18$ these corrugations appear to be negligible. If one considers a rail limiter in WENDELSTEIN VII-AS at $\varphi = 36^o$ and with a vertical dimension $Z_L = \pm$ 36 cm, the configurations are bound by a separatrix for $\iota > 0.45$. The right column of Fig. 13 shows configurations, where $\iota$ = 1/3 = 5/15 (top) or $\iota$ = 1/2 = 5/10 (middle and lower pictures) are at rational values within the magnetic topology. Here "natural" islands are seen in a poloidal chain. This is a peculiarity already

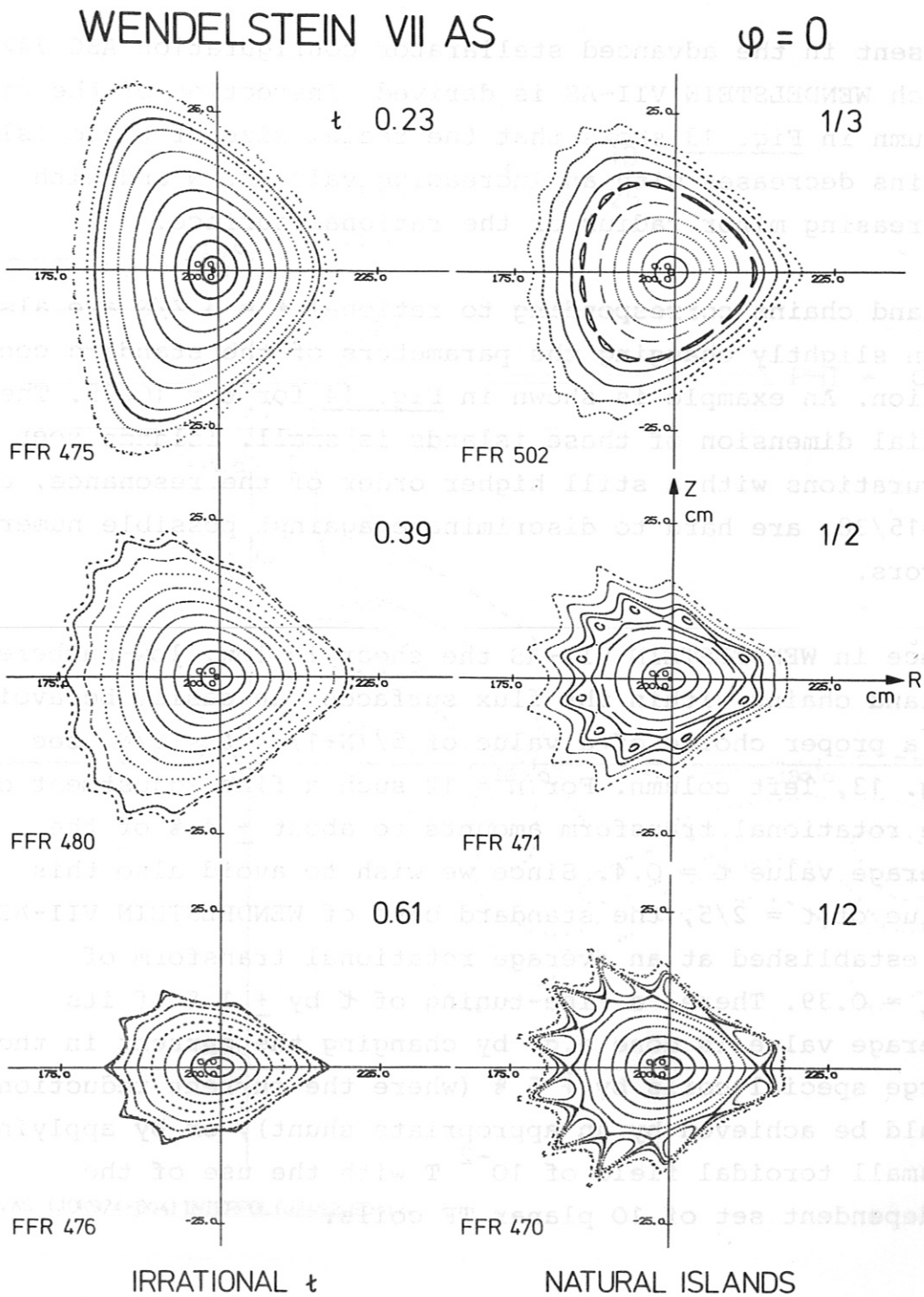


Fig. 13: Magnetic flux surfaces at various values of the rotational transform, toroidal position $\varphi$ = 0. Left column: irrational $\iota$, right column: examples of "natural" islands $\iota$ = 5/N for integer N = 10 and 15 within the configuration.

present in the advanced stellarator configuration ASC 742, from which WENDELSTEIN VII-AS is derived. Inspection of the right column in Fig. 13 shows that the radial size of these island chains decreases with an increasing value of N and with decreasing minor radius of the rational surface.

Island chains corresponding to rational $\iota = 5\ Z/N$ are also seen, when slightly changing the parameters of the standard configuration. An example is shown in Fig. 14 for $\iota = 10/25$. The radial dimension of these islands is small. Islands seen in configurations with a still higher order of the resonance, e.g. $\iota = 15/38$, are hard to discriminate against possible numerical errors.

Since in WENDELSTEIN VII-AS the shear is low, low-numbered island chains within the flux surfaces can easily be avoided by a proper choice of a value of $5/(N+1) < \iota < 5/N$, see Fig. 13, left column. For N = 12 such a fine adjustment of the rotational transform amounts to about $\pm$ 4 % of the average value $\iota = 0.4$. Since we wish to avoid also this value of $\iota = 2/5$, the standard case of WENDELSTEIN VII-AS is established at an average rotational transform of $\iota_{av} = 0.39$. There, a fine-tuning of $\iota$ by $\pm$ 1 % of its average value is done e.g. by changing the current in the large special coils by $\mp$ 5 % (where the current reduction could be achieved by an appropriate shunt), or by applying a small toroidal field of $10^{-2}$ T with the use of the independent set of 10 planar TF coils.

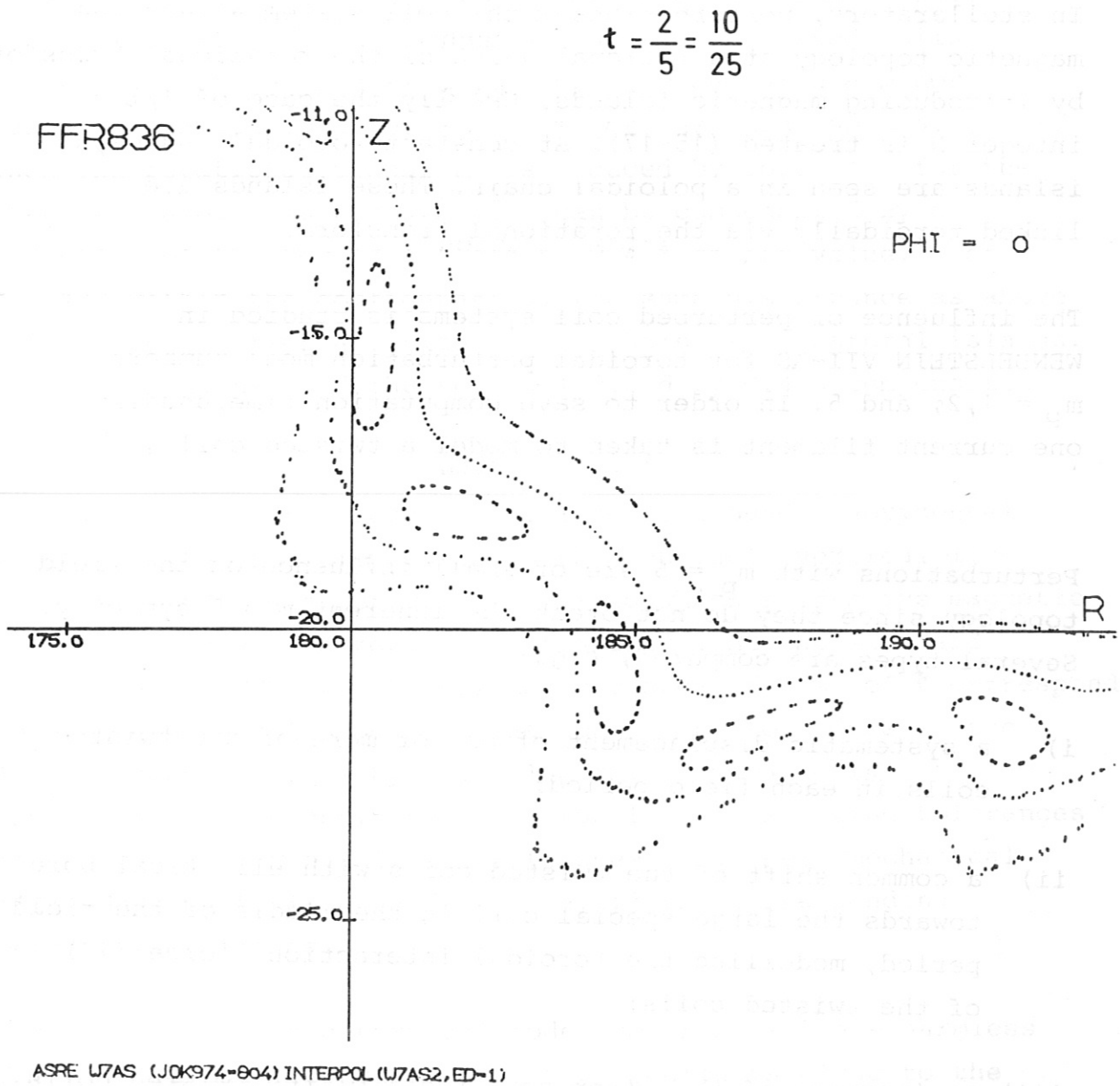


Fig. 14: Enlarged part of magnetic surfaces with chain of 25 islands corresponding to $t$ = 10/25; with parameters slightly different from the standard case.

PERTURBED COIL SYSTEMS

In stellarators, perturbations of the coil system affect the magnetic topology at a rational value of the rotational transform by introducing magnetic islands. Usually the case of $1/\iota$ = integer N is treated (15-17). At constant toroidal angles, N islands are seen in a poloidal chain. These islands are linked toroidally via the rotational transform.

The influence of perturbed coil systems is studied in WENDELSTEIN VII-AS for toroidal perturbation mode numbers $m_p$ = 1,2, and 5. In order to save computation time, usually one current filament is taken to model a twisted coil .

Perturbations with $m_p$ = 5 are of small influence on the field topology since they do not break the inherent m = 5 symmetry. Several types are compared, e.g.:

i) a systematic displacement of one or more of the twisted coils in each field period;

ii) a common shift of the twisted coils with elliptical bore towards the large special coil in the middle of the field period, modelling the toroidal interaction force (12) of the twisted coils;

iii) an increase of the minor coil radii of the twisted coils, which is caused by the electromagnetic hoop force and by the temperature increase during the pulse time of magnetic field;

iv) a common tilt of the large special coils.

In these perturbations the toroidal field components of WENDELSTEIN VII-AS are nearly maintained. From the change of the poloidal fields, or from locally varying radial or vertical fields a small change of the rotational transform is seen.

In order to model the transient behaviour of the twisted coils during the pulse time of about 5 sec we consider a relative toroidal shift of 2 mm between neighbouring twisted coils towards the large special coil, superimposed with a minor radius expansion of 2 mm, and 4 mm for the large special coils. Then the rotational transform is reduced by about 1 % for the standard case. This perturbation can be compensated by a reduction of the toroidal field by 0.4 % of its value. For $\iota = 1/2$ within the configuration, the same disturbance as above shifts the position and size of the chain of 10 natural islands. Again, a reduction of the toroidal field by 0.4 % compensates this change.

A common tilt of the large special coils around a horizontal axis, directed radially outwards through their vertical mid-plane, introduces a net vertical field which shifts the magnetic axis and changes the rotational transform. At the standard conditions of WENDELSTEIN VII-AS, a change of 1 % of $\iota$ corresponds to a lateral displacement of the top and bottom edges of the 5 large special coils by about 1.2 mm. This value is comparable to the estimated construction and mounting tolerances of those coils. Provisions are foreseen for their mechanical fine adjustment, in an effort to avoid the corresponding perturbation fields.

Perturbations with a toroidal mode number $m_p = 2$ are harmless for $\iota = 1/2$ but "resonate" at $\iota = 2/5$, which is close to the rotational transform of the standard case. As an example, an elliptic displacement of the major radii of the large special coils by 5 mm is considered. It produces a pattern of $m_p/\iota = 5$ islands with a radial extension of about 15 % of the radius of the enclosing flux surface, see Fig. 15, upper part. On the other hand, a homogeneous horizontal field $B_x = 0.1$ % of the toroidal field introduces 10 islands of similar size, but in a poloidally rotated pattern, as shown in the middle part of Fig. 15. Since here the perturbation mode number is $m_p = 1$, the resonance occurs evidently at $\iota = (m - m_p)/2m = (5 - 1)/10 = 2/5$.

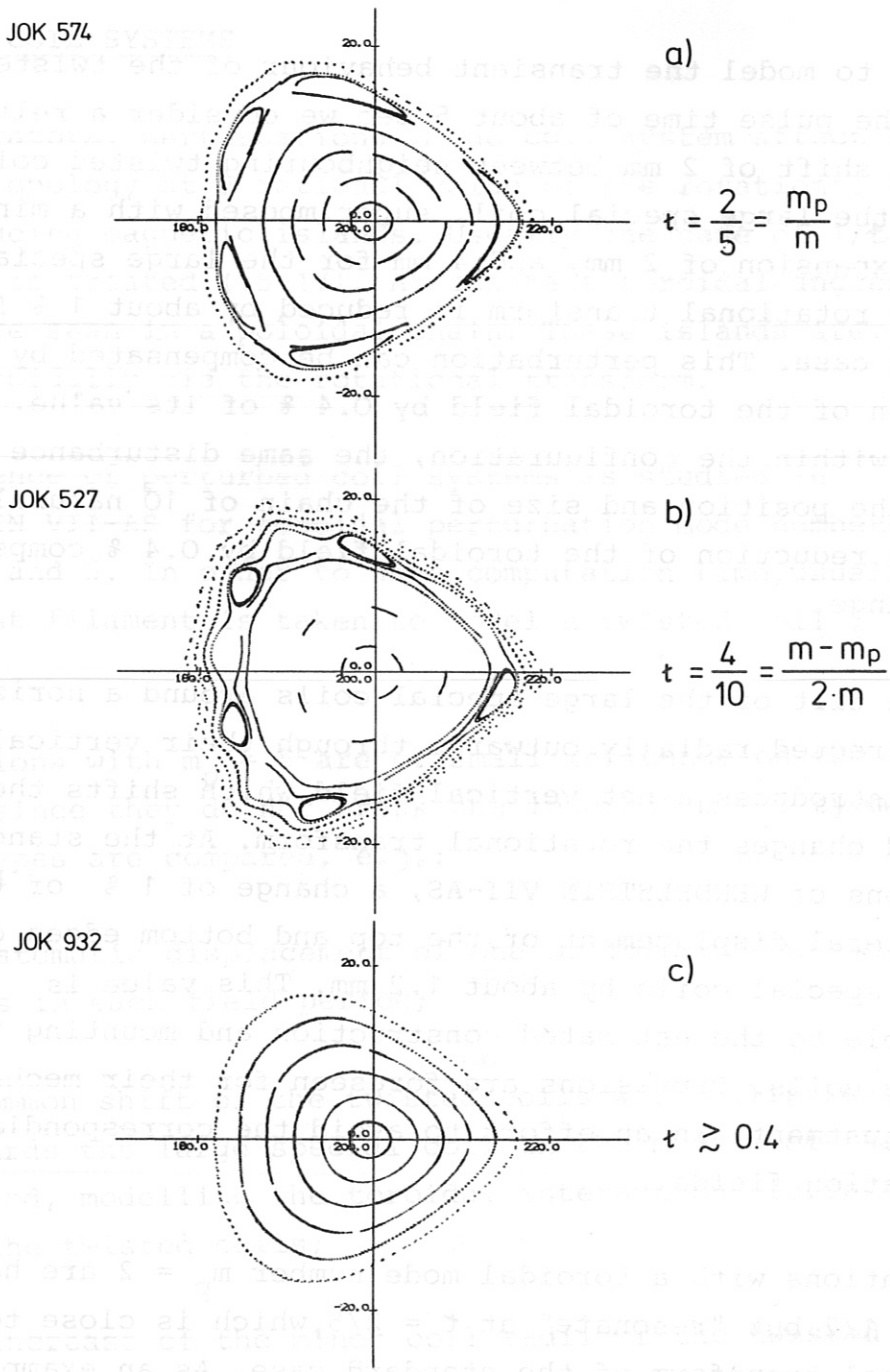


Fig. 15: Rotational transform near $t$ = 2/5. From top to bottom:
a) 5 islands produced by an elliptic displacement of the major radii of the large special coils ($m_p$ = 2);
b) 10 islands produced by a homogeneous field $B_x$ = 0.1 % of the toroidal field ($m_p$ = 1);
c) same disturbance as a), and toroidal field reduced by 0.2 % of its value in order to avoid the resonance.

When keeping the m = 2-perturbation and decreasing the toroidal field by about 0.2 % of its value, the 5 islands disappear, see bottom part of Fig. 15. Then, within the whole range of the flux surfaces, the rotational transform is above 0.4. A similar situation should apply for an appropriate increase of the toroidal field by reducing $\iota$ below the critical value of the resonance.

The behaviour of islands is studied in more detail for $\iota = 1/2$, and a toroidal perturbation mode number $m_p = 1$. Usually the two islands associated with this type of disturbance are the largest to be observed. The influence of different types of perturbation, like a change in the toroidal excursion of the current path, or a shift of one of the twisted coils or of the toroidal field coil system is scaled by comparing the position and size of the islands to their values at a homogeneous horizontal field $B_x$. This comparison is shown in Fig. 16. In WENDELSTEIN VII-AS, with increasing perturbation amplitude the 10 "natural" islands corresponding to $\iota = 1/2$ merge to groups of larger islands enclosed by additional internal separatrices. Some examples are shown in Fig. 17. Here, the unperturbed configuration at $\iota = 1/2$ is compared to cases, where the toroidal excursion of a twisted coil is reduced by 2 mm, and where the center of the 10 planar coils is displaced by 5 mm in the y-direction. The pattern in the lower right of Fig. 17 corresponds to an island structure obtained by a homogeneous horizontal field $B_x$ of $10^{-4}$ of the toroidal field.

Perturbations corresponding to a horizontal field $B_x$ larger than $(2 - 3)\ 10^{-4}$ of the toroidal field of WENDELSTEIN VII-AS should be avoided at $\iota = 1/2$. Such perturbations with toroidal mode number $m_p = 1$ would be caused, if one of the twisted coils with elliptic bore would have a toroidal excursion reduced by 5 mm, or would be toroidally displaced by 15 mm. A similar situation would occur if one of the large special coils would have a reduced toroidal excursion of 3 to 4 mm or an increase of its

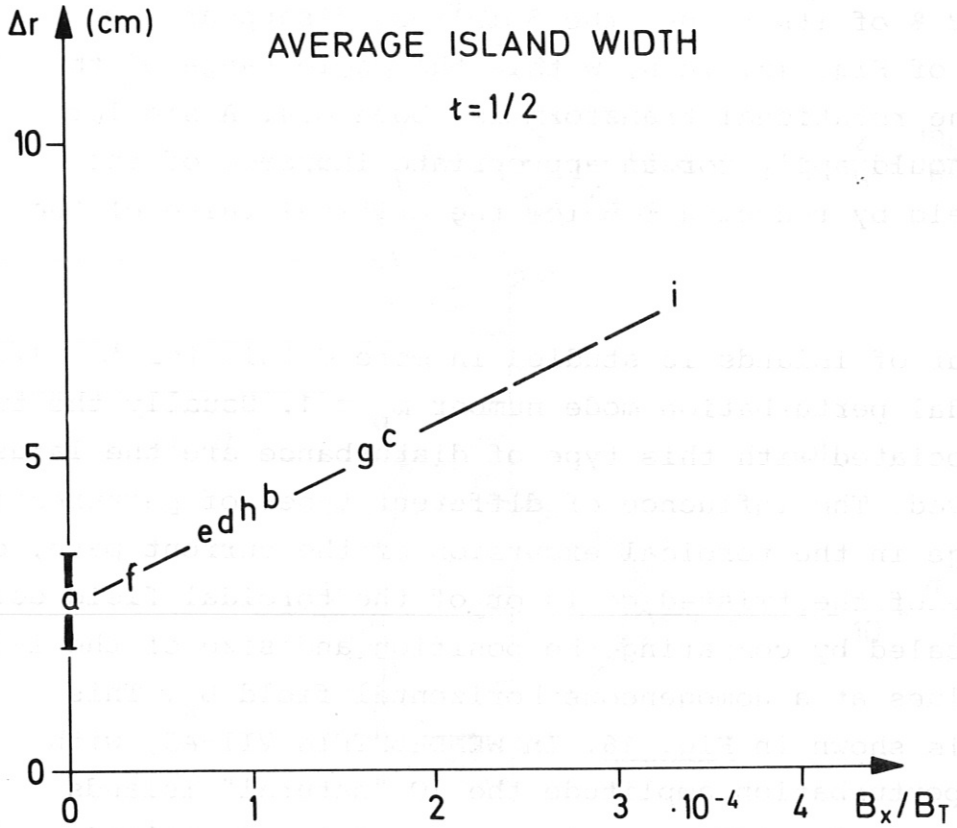


Fig. 16: Average radial size Δr of magnetic islands at $\iota$ = 1/2:

a) "natural" islands without perturbation

b) one twisted coil No 1: reduced toroidal excursion by 2 mm

c) one twisted coil No 1: toroidal shift of coil by 1 mm

d) one twisted coil No 9: reduced toroidal sxcursion by 1 mm

e) one large special coil: increased toroidal excursion by 1 mm

f) one large special coil: increased minor radius by 2 mm

g) System of 10 planar TF-coils: radial shift of center by 5 mm with respect to the center of the twisted coils

h) homogeneous horizontal field $B_x = 10^{-4}$ of toroidal field

i) as h), $B_x = 3.3 \times 10^{-4}$ of toroidal field

Δr is obtained as difference of the average radii of the inner and outer closed magnetic surface just encircling the magnetic islands.

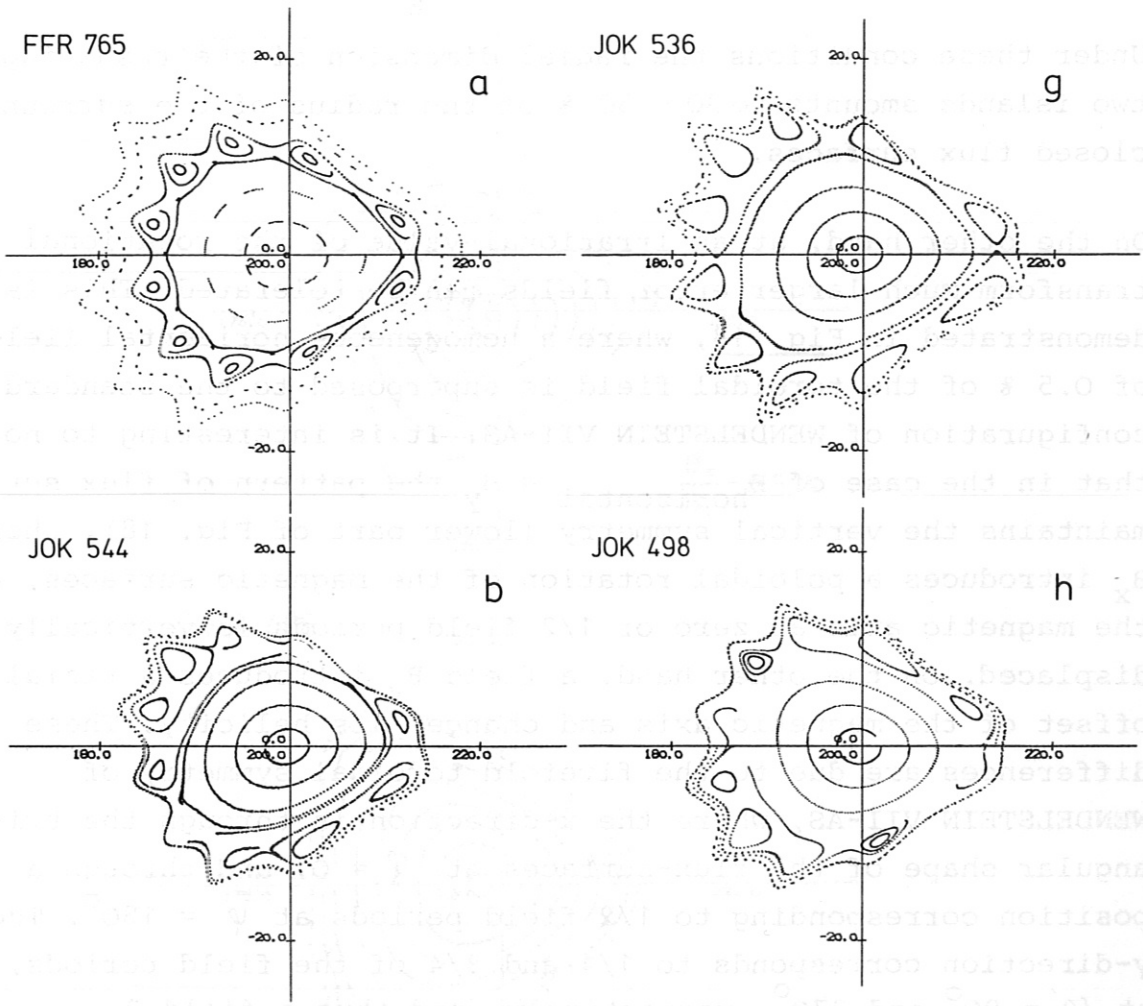


Fig. 17: Magnetic islands in WENDELSTEIN VII-AS at $\iota = 1/2$: unperturbed configuration with 10 "natural" islands, and three perturbed cases with $m_p = 1$: Cases a, b, g, and h of Fig. 16.

minor radius by 15 mm, or if the whole system of the 10 planar toroidal field coils would be radially offset by about 8 mm.

Under these conditions the radial dimension of the resulting two islands amounts to 30 - 50 % of the radius of the surrounding closed flux surfaces.

On the other hand, at an irrational value of the rotational transform much larger error fields can be tolerated. This is demonstrated in Fig. 18, where a homogeneous horizontal field of 0.5 % of the toroidal field is superposed to the standard configuration of WENDELSTEIN VII-AS. It is interesting to note that in the case of $B_{horizontal} = B_y$ the pattern of flux surfaces maintains the vertical symmetry (lower part of Fig. 18), whereas $B_x$ introduces a poloidal rotation of the magnetic surfaces, and the magnetic axis at zero or 1/2 field periods is vertically displaced. On the other hand, a field $B_y$ introduces a radial offset of the magnetic axis and changes its helicity. These differences are due to the fivefold toroidal symmetry of WENDELSTEIN VII-AS, where the x-direction is through the triangular shape of the flux-surfaces at $\varphi = 0$, and through a position corresponding to 1/2 field periods at $\varphi = 180^{\circ}$. The y-direction corresponds to 1/4 and 3/4 of the field periods, at $\varphi = 90^{\circ}$ and $270^{\circ}$, respectively, and thus a field $B_y$ interacts differently with the stellararator configuration.

Apart from a slight change in the rotational transform, a reduction in the size of the last useful flux surface in seen, amounting to 15 % for the above example.

If one wishes to keep this reduction below 5 %, i.e. below 1 cm of the effective minor radius, then the equivalent horizontal error field is to be kept below 0.2 % of the toroidal field. This would allow tolerances larger by about one order of magnitude than those stated above for the case of $\iota = 1/2$.

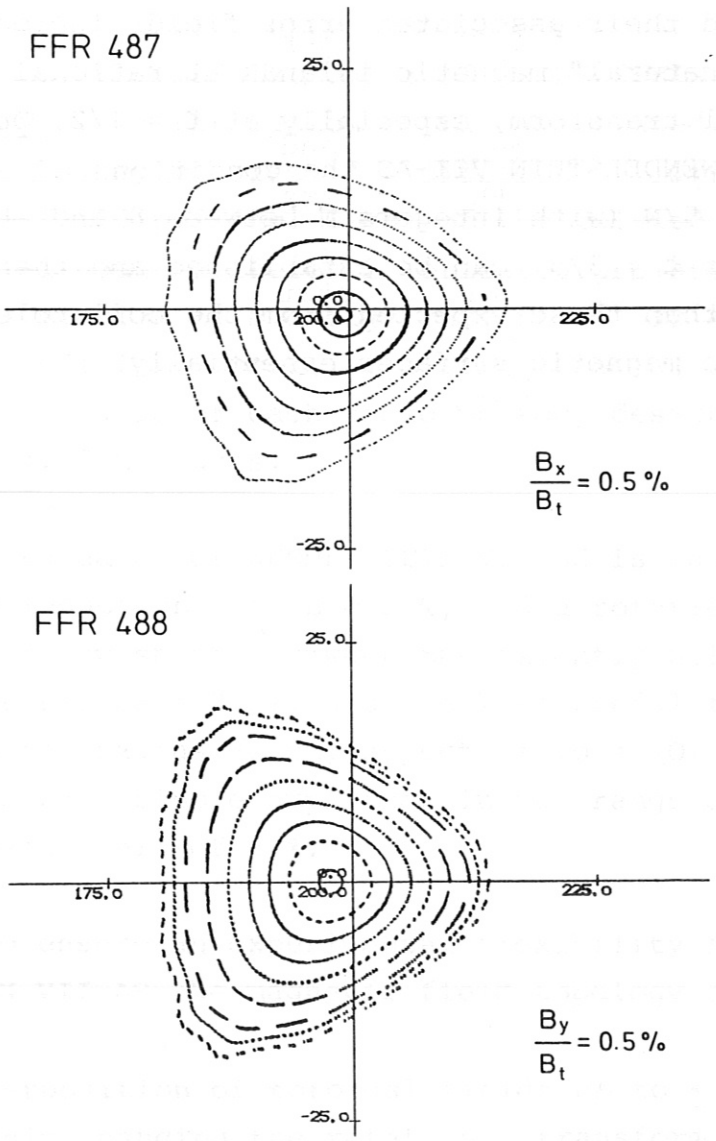


Fig. 18: Homogeneous horizontal fields $B_x$ (top) and $B_y$ (bottom) of 0.5 % of the toroidal field, superposed to the standard configuration of WENDELSTEIN VII-AS.

In conclusion: The motion of the coils caused by the electromagnetic forces and thermal expansion introduces only negligibles effects on the magnetic topology. Estimated coil tolerances and their associated error fields increase the size of the "natural" magnetic islands at rational values of the rotational transform, especially at $\iota = 1/2$. Due to the low shear in WENDELSTEIN VII-AS the conditions of $5/(N+1) < \iota < 5/N$ (with integers N between 8 and about 18) and $\iota \neq 2/5$ or $\iota \neq 3/5$ can be established and then larger error fields than those expected from the coil tolerances do not affect the magnetic surfaces essentially.

SUMMARY

Starting from the field of an advanced stellartor configuration, the modular coils of WENDELSTEIN VII-AS are developed by a discretization of the associated surface current distribution. They consist of 9 different twisted coils in each of the five field periods. Eight of the twisted coils are of identical, although differently oriented prolate elliptical minor cross section at a design current of 592 kA-turns. For providing sufficient access, one large special coil is introduced in the middle of each field period, designed for a current of 1.48 MA-turns.

The "standard case" of WENDELSTEIN VII-AS is characterized by an average induction of B = 3 T, and a rotational transform $\iota$ = 0.39 with low shear. Between the slightly helical magnetic axis (major radius = 2 m), and the last useful flux surface (average minor radius 20 cm, aspect ratio = 10) the magnetic field exhibits a ripple amplitude in the range of 1.5 to 15 % and a magnetic well of 2 %.

In order to ensure an experimental flexibility for WENDELSTEIN VII-AS the magnetic field topology can be varied by

i) superposition of toroidal fields up to $\pm$ 0.5 % T, mainly changing the rotational transform,

ii) by a vertical field up to $\pm$ 0.05 T, mainly changing the position of the magnetic surfaces, and influencing the magnetic well depth, or

iii) by an independent variation of the current in the large special coils, mainly influencing the magnetic ripple.

The rotational transform can be changed between $0.2 < \iota < 0.6$. The configurations are bound by a separatrix for $\iota > 0.45$. The aspect ratio of the magnetic surfaces increases with $\iota$ to values of about 20 at $\iota = 0.6$ .

At rational values of $\iota = 5/N$ "natural" magnetic islands occur within the system of closed flux surfaces in a poloidal chain of N islands.

Effects of magnetic perturbations are studied for toroidal mode numbers $m_p = 1,2,$ and 5. At rational values of $\iota$, e.g. 1/2 or 2/5, the magnetic surfaces are perturbed by magnetic islands. Such perturbed configurations can be avoided by operation at values of the rotational transform where $5(N+1) < \iota < 5/N$ (with N between 8 and 18) and at $\iota \neq 2/5$ or $\iota \neq 3/5$. There the magnetic surfaces are not affected by perturbations, except for some reduction of the separatrix radius. From these studies estimates of the admissible tolerances of coil construction or coil mounting are derived.

REFERENCES

(1) Joint US-EURATOM-Report:
STELLARATORS, Status and Future Directions
Max-Planck-Institut für Plasmaphysik, Report IPP 2/254,
July 1981, Chapter V.2

(2) R. Chodura et al., IEEE Transact. on Plasma Science,
Vol. PS-9, No. 4, Dec. 1981, 221

(3) F. Rau, et al., Proc. 9th Europ. Conf. on Contr. Fusion
and Plasma Physics, Oxford 1979, Vol. I, 76 and Vol. II,
547

(4) W. Lotz et al., Proc. Annual Meeting on Theoret. Aspects
of Contr. Thermonucl. Res. Austin 1981, paper 3B41

(5) F. Rau, et al., Verh. DPG, 4/1982, 513, paper P49

(6) H. Wobig, et al., Verh. DPG, 4/1982, 499, paper P17

(7) WENDELSTEIN VII-AS, Application for EURATOM
PREFERENTIAL SUPPORT - Phase I, December 1981 (unpublished)

(8) Max-Planck-Institut für Plasmaphysik, Garching
Annual Report 1981

(9) U. Broßmann et al., to be published in Proc. of 9th Int.
Conf. on Plasma Physics and Controlled Nuclear Fusion
Research, Baltimore 1982

(10) W. Dommaschk, Max-Planck-Institut für Plasmaphysik,
Garching, Report IPP O/38, 1978

(11) W. Dommaschk, Z. Naturforsch, Vol 36 a, 1981, 251

(12) U. Broßmann, et al., "Mechanical Stress Analysis ..." Proc. 12th SOFT 1982, Jülich, to be published

(13) U. Broßmann, et al., "Modular Mechanical Design ..." Proc. 12th SOFT 1982, Jülich, to be published

(14) J. Sapper, et al., "The Advanced Stellarator WENDELSTEIN VII-AS", Proc. 12th SOFT, to be published

(15) C. Gourdon, et al., Proc. 3rd Int. Conf. on Plasma Physics and Controlled Nuclear Fusion Research, Novosibirsk, 1968, 847

(16) S. Rehker, H. Wobig, Proc. 8th SOFT 1974, Jutphaas, 221

(17) F. Rau, et al., Max-Planck-Institut für Plasmaphysik, Garching, Report IPP 2/231, 1976